

Estimating the Monostatic RCS of Variable Ratio Pylons Using MoM with Localized Meshing

P. Mark Ingerson, and Vince Rodriguez, *Fellow*

EM Analysis Group
NSI-MI Technologies
Suwanee, GA, USA

Vince.Rodriguez@AMETEK.com

Abstract— Larger low-observable targets are being mounted onto RCS pylons. In many cases not only Azimuth rotation of the target, but a degree of movement in elevation is desired. This requires in many cases a large number of positioning cables to run from the base of the pylon to the tip where the rotator is placed. At the same time the low-observable qualities of the target call for pylon ogives with higher ratios to minimize the background RCS of the pylon that supports the target. The higher ratios call for very thin structures that cannot handle the weight of the rotator or have not enough space for the control and power cable to be fed to the rotator. A way of solving this problem is to have a variable ratio pylon, where the ogive at the tip is different from the ogive on the main body of the pylon. To analyze these pylons a higher-order basis-function method of moments (HOBFMoM) approach has been used in the past [1]. To conform the quadrilateral flat patches to the round geometry of the pylon, patches smaller than 0.3λ were used. While this was still an advantage over the typical 0.1 to 0.05 λ patches it placed limits on the highest frequencies that could be analyzed give the available computational resources. In this paper the authors present an approach to the meshing of the structure that allows for computing the monostatic RCS at frequencies in the x-band for a 2.4 m tall pylon. In addition, the effects of the non-physical absorber terminations are further analyzed.

I. INTRODUCTION

To measure RCS, specialized positioners are designed to support the target. These devices can be based on having a low dielectric property, close to air, such as expanded polystyrene (EPS) columns [2]. Baggett and Thomas [2] discuss some of the drawbacks of the foam column as a support. The foam columns have a limited weight that they can support while maintaining a permittivity that is close to air. Higher density foams, used to support higher loads, have higher permittivity. In reference [2] it was shown that the RCS of the Styrofoam column increased from -40dBsm (dB related to a square meter) at 2 GHz to levels in the -21dBsm range at the upper end of the K band. The column measured in [2] could support TUTs of up to 22.68 kg (50 Lbs.). RCS metallic pylons can support much higher loads. Models that support up to 1364 kg (3000 lbs.) are shown in [3]. Hess describes in [4] that the typical RCS pylon has the cross section of two intersecting circles that describe an ogive. The length to width ratio describes the geometry of the ogive. In [3, 4] typical ratios of 4 to 1 are mentioned, but ratios of 6:1 and even higher have been implemented. There is a limit to the ratios that can be

physically achieved. Designing the pylon so that it does not bend under load limits the ratios that can be used. The target needs to be rotated to measure the RCS from different angles of arrival. This rotation requires a rotator at the top of the pylon and the ogive width is limited to allow electrical power and feedback cables for the mechanical systems that rotate the target.

A compromise is a variable ratio pylon. These pylons change to lower ratios as they approach the tip to allow for cables to pass through and also to have a level of thickness that will minimize bending under load. The effect of these variable ratio pylons on the RCS measurement has to be studied. In [1], data was presented for the RCS of a pylon using a non-physical absorber termination to avoid the effects of the pylon end (which is hidden by the target during measurements), and also to terminate the geometry when modeling a finite pylon. The highest frequency analyzed in [1] was 3 GHz. The limit was determined by the computational resources available and the large number of unknowns required. The mesh size was set such that the quadrilaterals that represent the geometry were about 0.3λ at the highest frequency being solved.

In this paper the mesh is optimized and different features are modeled with different mesh constraints. Patches as long as 1.8λ can be used. The first step is to validate the meshing approach. This is done by modeling a squat cylinder. Squat cylinders are the typical geometry used to calibrate RCS ranges [5-7].

II. SQUAT CYLINDER ANALYSIS

The 1800 and the 900 squat cylinders are computed to obtain the monostatic RCS. The 1800 cylinder is 45.72 cm (18 in.) in diameter and 21.336 cm (8.4 in) in height. The 900 cylinder is 22.86 cm (9 in.) by 10.67 cm (4.2 in). Symmetry planes are used to reduce the size of the structure. One set of simulations uses patches that are 0.3λ in size, as it was done on [1]. The λ value is at the at the highest frequency being simulated, which happens to be 6 GHz for the 1800 cylinder and 10 GHz for the 900 cylinder. The other simulation uses patches that are up to 1.8λ for the top surface. The cylindrical surface is set to have patches that are 1.8λ in length, but the angle between the patches is limited to 1.5 degrees.

The meshes created for the 1800 cylinder case are shown in Figure 1. The 0.3λ mesh required 6814 unknowns, while the optimized mesh requires 4892 unknowns, a 28% reduction in

unknowns. The solver time also experienced a reduction of 8.5%. More importantly, the results of the reduced mesh are the same as those of the 0.3λ mesh; there is no additional error from using the localized meshing.

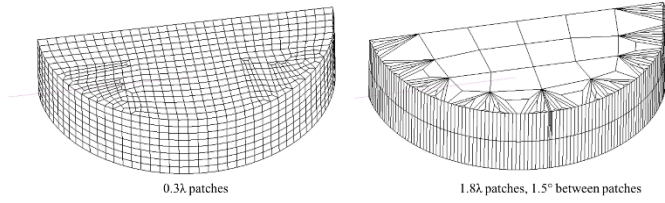


Figure 1. The mesh created for solving the RCS of the squat cylinder using the HOBf-MoM.

Figure 2 shows the RCS results for the two meshing approaches and for the two cylinders analyzed. The results agree with the ones presented [5-7]. While the savings in time and number of unknowns may seem small, for the pylon geometry the reduction is much greater, given the elongated geometry of the pylon.

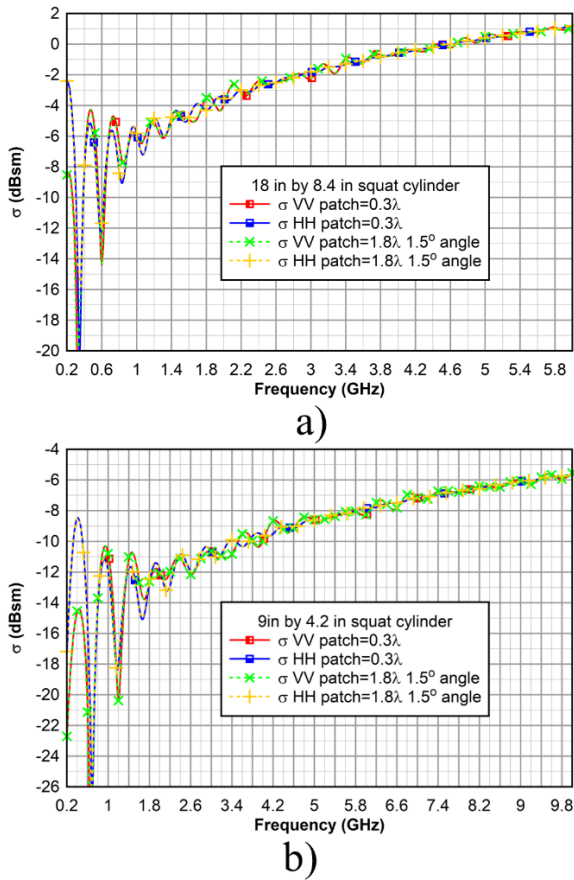


Figure 2. Monostatic RCS results for squat cylinders for both polarizations. For the 1800 cylinder a) and for the 900 cylinder b).

The results shown on Figure 2 demonstrate that properly adjusting the angle between the patches when modeling a curve while maintaining a large size (i.e. 2 or 1.8λ) to take advantage of the higher order basis functions provides the same results as

using a smaller patch, as was done in [1]. Now that the approach has been validated by analyzing squat cylinders, the same technique is applied to the analysis of the pylons.

III. PYLON ANALYSIS

The pylon analyzed has a variable ratio. At the very bottom of the structure the pylon has a 6:1 ratio. This ratio is preserved along the length of the pylon, but as we approach the tip the structure blends into a 5:1 ratio. This allows for a high ratio over most of the length of the pylon and a lower ratio at the tip where a thicker pylon is needed to pass cables and reduce bending under load.

A. Geometry Being Analyzed

Figure 3 shows the geometry of the pylon section being analyzed. As was done in [1], only a section of the pylon is analyzed. This section would be illuminated by the compact range reflector, and it includes the section that resides inside of the quiet zone [1]. The vertical dimension of the modeled pylon section is 2.59 m and it is analyzed up to 10 GHz. At that frequency the height of the model is over 86 wavelengths. This is an electrically very large problem. Symmetry will help in reducing some of the unknowns required to solve the problem. The HOBf-MoM allows for using patches up to 2λ in length, thus reducing the number of elements needed to discretize the geometry.

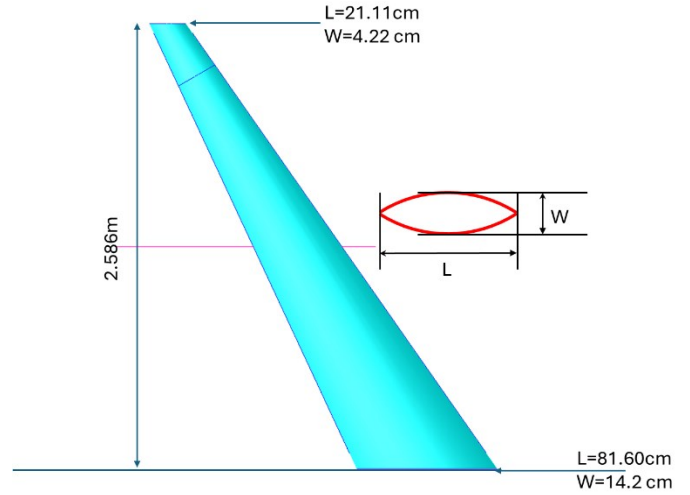


Figure 3. the geometry of the pylon being analyzed.

The pylon is modeled as a perfect electric conductor (PEC). As it was done in [1], a non-physical absorber ogive is placed at the base and the tip of the pylon model. The lossy ogives are used to hide the effects of the truncation of the pylon [1]. The lossy ogive material is defined by:

$$\begin{aligned}\epsilon_r &= 1 + j10 \\ \mu_r &= 1 + j10\end{aligned}\quad (1)$$

This material has the same wave impedance as free space so the termination ogives have a minimal RCS. This, in addition to

their ogive shape, reduces the RCS [8] for the angle of arrival being analyzed.

B. Model Meshing

The pylon is a very long structure with an almost flat, very shallow surface curve in one direction (longitudinally), and a more pronounced curve profile in the orthogonal direction (transverse). This geometry makes it ideal for having long patches, up to 1.8λ in size along the length of the pylon. However the curved shape does not lend itself to long patches. These curved surfaces are the reason while in [1] the patch size was reduced to 0.3λ . However, if the patch size is set to a maximum of 1.8λ , but the angle between the patches is set to a maximum of 1.5° , the meshing process will create narrow patches with denser boundaries along the tighter surface curve and a better mesh can be obtained that uses fewer unknowns at a given frequency to model the geometry.

Figure 4 shows the mesh for the pylon using the different meshes. The original mesh used in [1] set the elements to a maximum size of 0.3λ . This constraint results in an extremely dense mesh that is shown on the left side on Figure 4. For the present paper, the mesh differed, depending on the materials that form the boundary where the integral equations are solved. Also the shape of the structure is taken into account.

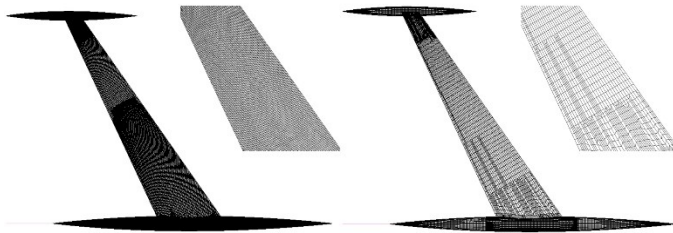


Figure 4. different meshing approach for the pylon, the left pylon model uses 0.3λ and the right model using the optimized mesh.

For the PEC to air boundaries (mainly the pylon itself) the patch elements size was set to 1.8λ , as was done for the squat cylinders. The largest angle between the mesh elements was also set to 1.5° . The air-to-non-physical-absorber boundaries are on the lossy ogives. There, setting the angle between patches to 1.5° creates a very large number of patch elements on those surfaces, so the largest angle between patches was instead set to 10° . Leaving the maximum dimension of the patch to 1.8λ created a poor approximation to the ogive curvature. Instead, a maximum size of 0.5λ was shown to give good results and provide a nice approximation to the curvature of the ogive. At 10 GHz, the entire structure can be modeled with a total number of 189,043 unknowns (electric and magnetic currents at the boundaries). The 0.3λ sized patch model required in excess of 1,500,000 unknowns, which is much higher than what the solver can handle. A total of 688,889 unknowns are required for 6 GHz, a frequency that is lower than the 10 GHz that was simulated with the localized mesh constrains.

C. RCS Results

Once the meshing was set, the model was run. The pylon with the termination ogives was run for vertical and horizontal

plane wave illumination and the monostatic RCS was computed. The simulation was executed from 600 MHz to 10 GHz. Figure 5 shows the RCS results for the geometry. A separate simulation was performed using the lossy ogives by themselves, as was done on [1], to establish a “noise floor” for the simulation. The results, shown in Figure 5, agree with the expected levels for these pylon ratios. RCS levels for the pylon that are smaller than -50dBsm are achieved from 4 GHz and above. Levels of -60dBsm are achieved above 6.5 GHz for both principal polarizations.

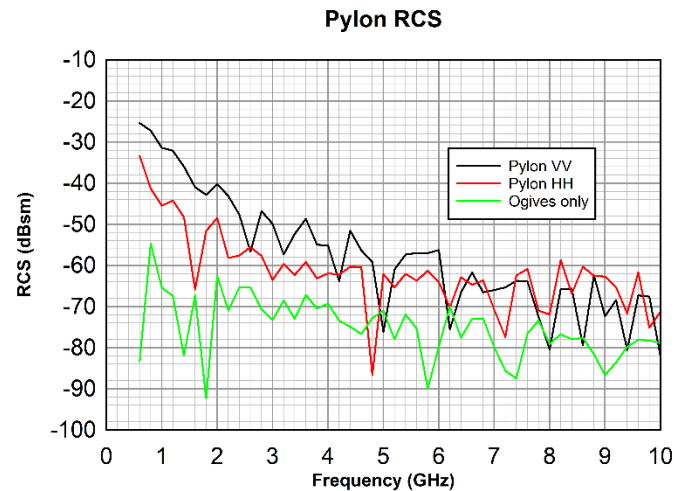


Figure 5. RCS of the pylon.

D. Effects of Lossy Ogives Embedding

The lossy ogives are created by using the cross section of the pylon at each end to create bodies of revolution about their longest dimension. The generated ogives are scaled in length and width [1] to eliminate the effects of the pylon edges. Following this approach, which was also done in [1], causes the pylon to be embedded in the lossy ogive, (see figure 6.) To verify that this embedding has a minimal effect on the computed RCS, the ogives were shifted so that the pylon is minimally embedded in the lossy ogives. Figure 6 shows how the ogives are shifted to minimize the embedding.

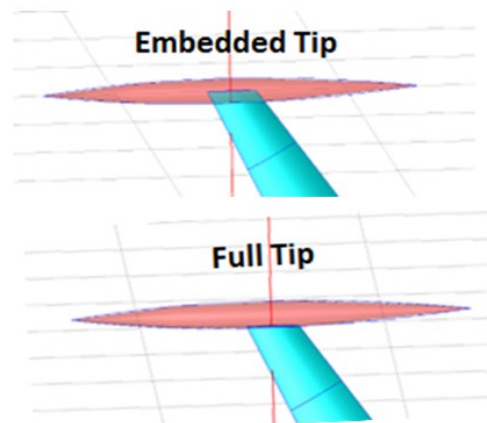


Figure 6. Embedding the pylon tip less into the ogive to provide full tip illumination by the incoming wave.

The simulations are repeated using the minimal embedding and compared with the previous results. Figure 7 shows the comparison of the results.

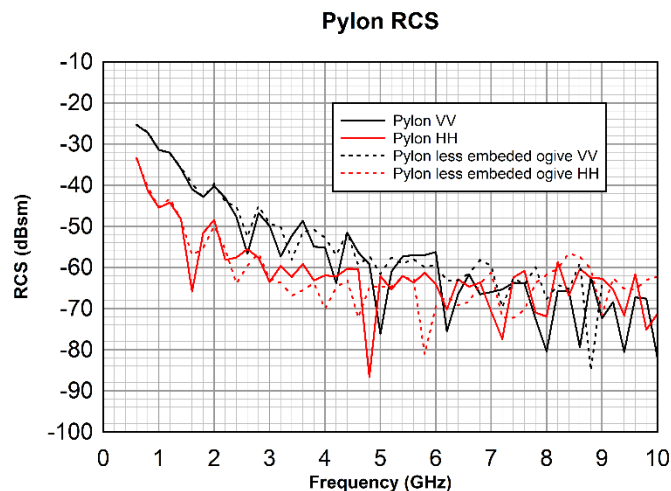


Figure 7. RCS of the pylon for different levels of ogive embedding.

The data on Figure 7 shows that the two different levels of pylon termination ogive embedding result in basically the same RCS. Remember that the for dB levels computed, the difference between -60 dBsm and -70 dBsm is 0.0000009 m² (0.9mm² or 0.0014 sq. in.), or -60.46dBsm.

IV. CONCLUSION

The technique that was introduced in [1] to model RCS pylons using the HOBf-MoM has been used in this paper, but rather than using a brute-force approach to the meshing and uniformly reduce the size of the patches to conform to the curved features of the structure, a more intelligent approach is presented where the patch shapes are elongated in the direction where the surface is flatter and they are narrowed in the direction where the surface is more curved. This is

accomplished by limiting the allowable angle between patches at their boundaries to better approximate a piecewise model to the curved surfaces. This efficient meshing allows for a solution at a much higher frequency than what was achieved using smaller patches. This approach was validated by looking at the RCS of standard calibration targets and it is believed that it is a suitable method for estimating the RCS of traditional pylons as well as those with variable ratios.

REFERENCES

- [1] V. Rodriguez, "Using a Non-Physical Absorber Termination for the Analysis of RCS Pylons Using a Higher Order Basis Function Method Of Moments," 2023 17th European Conference on Antennas and Propagation (EuCAP), Florence, Italy, 2023, pp. 1-4, doi: 10.23919/EuCAP57121.2023.10133548
- [2] M. Baggett and T. Thomas "Obtaining High Quality Measurements with a Very Large Foam Column" 27th Annual Meeting and Symposium of the Antenna Measurement Techniques Association (AMTA 2005), Newport, Rhode Island, October 2005
- [3] Scientific Atlanta Product Catalog "Microwave Measurements Systems and Products" Scientific Atlanta, Atlanta Georgia March 1996 pp. 150-152.
- [4] D. Hess, "Introduction to RCS Measurements" 2008 Loughborough Antennas & Propagation Conference, Loughborough, UK, 17-18 March 2008, pp. 38-44
- [5] B. M. Kent, and W. D. Wood Jr. "The Squat Cylinder and Modified Bicone Primary Static RCS Range Calibration Standards" 19th Annual Meeting and Symposium of the Antenna Measurement Techniques Association (AMTA 1997), Boston, Massachusetts, November 17-21, 1997 pp 319-324.
- [6] P. S. P. Wei, A. W. Reed, C. N. Ericksen and R. K. Schuessler, "Measurements and Calibrations of Larger Squat Cylinders," in IEEE Antennas and Propagation Magazine, vol. 51, no. 2, pp. 205-212, April 2009
- [7] X. Xu, Z. Xie and F. He, "Fast and Accurate RCS Calculation for Squat Cylinder Calibrators [Measurements Corner]," in IEEE Antennas and Propagation Magazine, vol. 57, no. 1, pp. 33-41, Feb. 2015.
- [8] A. C. Woo, H. T. G. Wang, M. J. Schuh and M. L. Sanders, "EM programmer's notebook-benchmark radar targets for the validation of computational electromagnetics programs," in IEEE Antennas and Propagation Magazine, vol. 35, no. 1, pp. 84-89, Feb. 1993.